HARMONIC TIDAL CURRENTS ASSOCIATED WITH THE INTERNAL TIDE IN GENKA BAY, OKINAWA

Muhammad Abdur ROUF[1] and Eizo NAKAZA[2]

[1]Member of JSCE, Doctoral Student, Dept. of Civil Engineering and Architecture, University of the Ryukyus (Senbaru 1, Nishihara chow, Okinawa 903-0213, Japan)

[2]Member of JSCE, Professor, Dept. of Civil Engineering and Architecture, University of the Ryukyus (Senbaru 1, Nishihara chow, Okinawa 903-0213, Japan)

沿岸・海洋の開発に係わるアセスメントにおいて，潮流予測は基本的な検討項目となっている．最近，数値計算的には三次元的な潮流解析が主流となりつつある．しかしながら，実測データに関しては，広範囲にまたがる3次元的なデータ取得が困難であり，現実的対応として，鉛直方向に観測点を１点設ける潮流観測が採用される場合が多い．特に，島嶼の小規模開発などにおいては，予算的な面からその選択肢がとられる場合が多い．

本研究においては，ADCPを用いた潮流の鉛直方向観測が，夏季と冬季に行われ，データの調和分解を通じて，水深平均された1層モデルと実際の流れとの比較が示されている．また，それらの相違が流速データのスペクトルにいかような形で現れるかが示され，内部潮汐の存在の存在との係わりが議論されている．その議論からは，内部潮汐の発達が想定される夏季においては，比較的沿岸部においても水深平均値として与えられる１層潮流モデルの適用が困難であることが示されている．

Key Words : *Harmonic tidal currents, internal tides; hydrodynamics; coastal engineering; Okinawa; Japan.*

1. BACKGROUND

Assessment of tidal phenomenon is prerequisite for any construction works such as port developments, land reclamation in coastal waters, and coastal protection works. In general, assessment of tidal phenomena is based on observation or numerical simulation. Three-dimensional concept for numerical simulation is becoming popular in recent years to assess the tidal hydrodynamics[1-2] but one-layer concept is still commonly used for engineering design in order to overcome high costs and computing time[3-4]. It is obvious that three-dimensional model or multi-layer observation provides more accurate results than that of one-layer model or depth-averaged observation. Detail of the inherent hydro-physical process, however, triggering that accuracy has not been sufficiently shown.

Internal tides are an important hydro-physical process in ocean dynamics and have a significant link in the chain of energy flux from tides to turbulence and internal waves of all frequencies and can intensify tidal currents. Internal tides are being discussed frequently in current research[5-7], but rarely in connection with the tidal current estimation processes. The present study, therefore, aims to know the considerable hydro-physical process and their seasonal behavior for deciding whether to use one-layer (depth-average) or multi-layer observation for estimating accurate tidal currents in Genka Bay.

2. METHODOLOGY

Field observations for the present study were carried out in Genka Bay, Okinawa. The main island of Okinawa and its surrounding seabed topography are presented in the upper right corner box in **Fig. 1**. The shelf region of the study area has a gradual slope with depths ranging from 25–110 m, whereas most of Okinawa Island borders narrower areas of the continental shelf. The coastline along the study area resembles a bay and is surrounded by intensive artificial constructions. The survey area including the three observation sites (St. 1, St. 2,

and St. 3) are also shown in **Fig. 1**. St. 3 is the observation site nearest to shore while St. 2 and St. 1 are farther offshore from the coast.

Acoustic Doppler Current Profilers (ADCPs) and Acoustic Doppler Profilers (ADPs) were deployed in the study area to obtain time series vertical profiles of horizontal velocities. The profilers were positioned in upward looking mode and were configured to sample at 10-min time intervals with a 2-meter depth bin for averaging. Measurements covered over 80% of the water column depth, including the center of the first and the last good data bins above the seabed. Towable, profilable, and moorable (TPM) chlorotec sensors (ALC2180, JFE Alec Co., Ltd.) were used during ship-based measurements of water temperature and density at all sites. They were deployed during the summer and winter seasons. A summary of the deployment periods and instrumentation is given in **Table 1**. Sea level data were obtained from the nearest meteorological station (Nago observatory). The location of the observatory is also marked on **Fig. 1**.

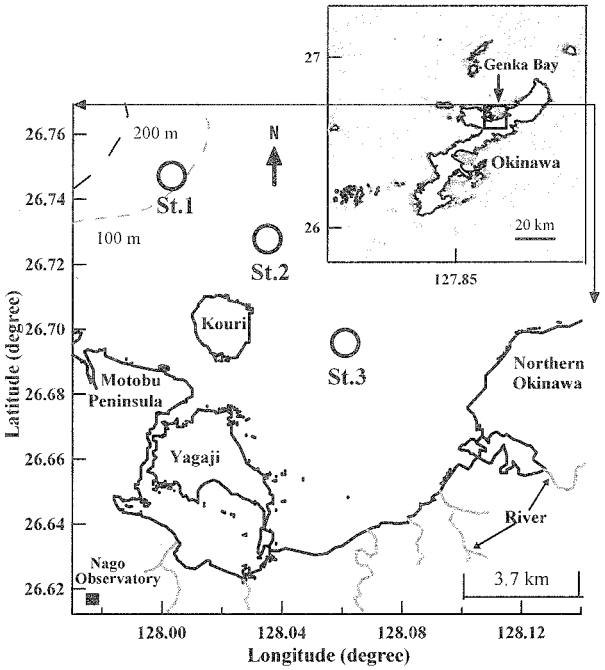

Fig.1 Seabed topography around Okinawa Island and observation sites of Genka Bay.

Harmonic tidal analysis, following Eq. (1) and considering eight major tidal constituents (M_2, S_2, N_2, K_2, K_1, O_1, P_1, and Q_1), was done based on a 30 day period of recorded current data for the calculated records.

$$h = H_0 + A_1 \cos(at + E - k)_1 + A_2 \cos(at + E - k)_2 \cdots A_8 \cos(at + E - k)_8 \quad (1)$$

where h = Height at any time t; H_0 = Height of mean water level above a selected datum; $A_{1,2\cdots8}$ = Amplitudes of the constituents; a = Frequency (speed); E = Equilibrium argument of a constituent at $t = 0$; and k = Phase lag or Epoch.

3. RESULTS AND DISCUSSIONS

(1) Distributions of observed and harmonic tidal currents

An attempt has been made in this section to portray and compare the measured and harmonic tidal currents at St. 2 during both summer and winter for depth-averaged phenomena.

Ten-minute interval time series of the measured sea level and depth-averaged currents for the east-west and north-south current components are

Table 1 Overview of instruments deployed in Genka Bay.

Mooring Sites	Position	Period	Dates	Observation Depth/Water Depth (m)	Instrument type
St. 1	26°44'49.92" N 128°6'10.8 W	Summer	September 9 – October 9, 2007	16–106/110	300 KHz ADCP (RD instruments)
		Winter	–	–	–
St. 2	26°43'40.08" N 128°2'6" W	Summer	September 9 – October 9, 2007	10–59/62	500 KHz ADP (NORTECK)
		Winter	November 8 – December 11, 2006	13–54/58	300 KHz ADCP (RD instruments)
St. 3	26°41'44.88" N 128°3'39.6" W	Summer	September 26 – October 26, 2007	15–48/50	600 KHz ADCP (RD instruments)
		Winter	–	–	–
St. 1, St. 2 and St. 3	–	Summer	September 28, 2007	St. 1:110, St. 2:62, St. 3:50	TPM Chlorotec sensors (ALC2180, JFE Alec Co. Ltd.)
		Winter	December 11, 2006	St. 1:94, St. 2:58, St. 3:38	

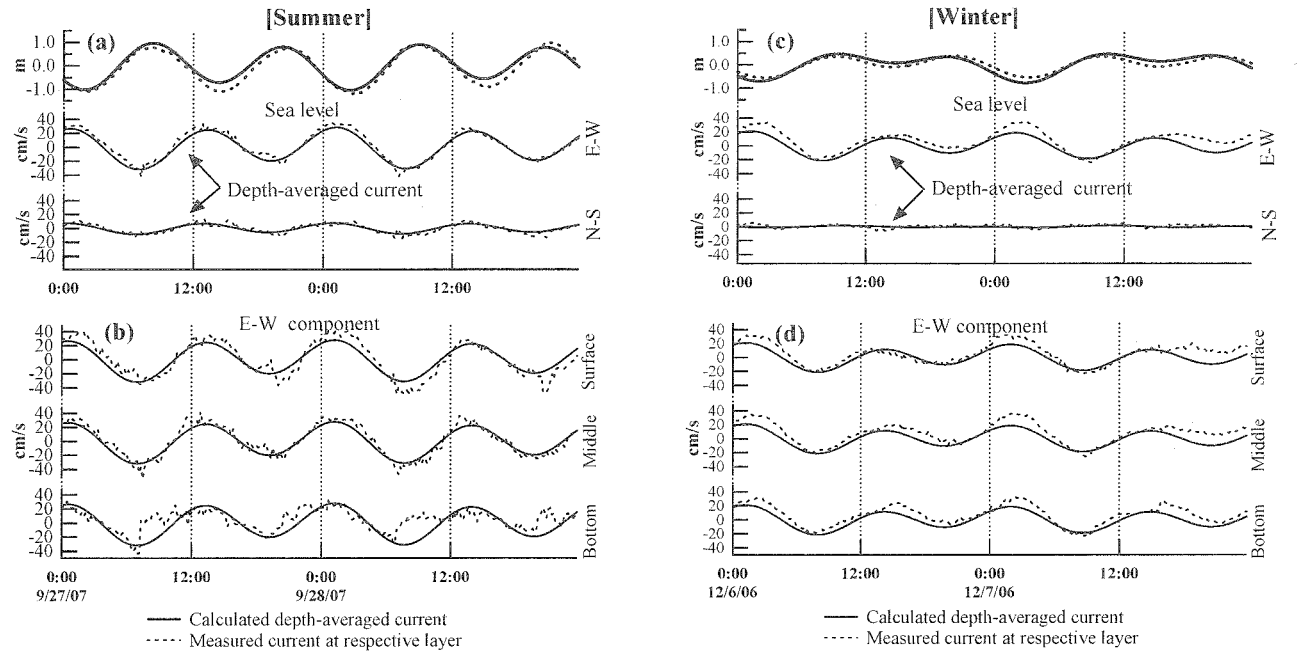

Fig.2 Comparison of measured and calculated records at St.2: Sea level and depth-averaged currents against the respective calculated records during (a) summer and (c) winter; Measured (surface, middle and bottom layer) currents against the calculated depth-averaged currents at E-W component during (b) summer and (d) winter.

plotted with their respective tidal-fitted (hereinafter called calculated) records for three representative days of the summer period in **Fig. 2(a)**. Hereafter, the east-west and north-south components are written as E-W and N-S, respectively. As shown in **Fig. 2(a)**, the measured sea level and depth-averaged records show good agreement with their respective calculated values. The sea level and depth-averaged currents, as well as their respective calculated records, show a similar semidiurnal oscillation pattern as expected. The E-W depth-averaged current shows stronger amplitude than the N-S depth-averaged current.

For a comprehensive assessment, the calculated depth-averaged records of the E-W components are plotted with the surface, middle and bottom layer measured records in **Fig. 2(b)**. The surface, middle and bottom layer represents 13, 29 and 54 m respectively, deep from the surface. The calculated depth-averaged and measured records at the surface and middle layers agree well but the component shows prominent disagreements in the bottom layer. Both the phases and the amplitudes of the measured records disagree with the calculated depth-averaged records in this bottom layer. N-S component also shows the similar notable feature like E-W and not shown in this paper.

Similar to the summer data, sea level and depth-averaged currents are plotted against their respective calculated records for three representative days of winter in **Fig. 2(c)**. As shown in **Fig. 2(c)**, the sea level and the depth-averaged values show good agreement with their respective calculated records as observed for the summer. Now, for comprehensive view, the calculated depth-averaged records of the E-W current component in winter are plotted against the surface, middle and bottom layer measured records in **Fig. 2(d)**. It is notable that the phases and amplitudes of the measured records in all the layers shows similar good agreement with their respective calculated depth-averaged records for the E-W component. Similar observation is also noticed in N-S component and not shown in this paper.

The calculated depth-averaged currents show similar agreement patterns with the measured currents in all three layers during the winter (**Fig. 2(d)**) but disagreement in the bottom layer currents during the summer (**Fig. 2(b)**). The sea level and depth-averaged currents, however, show good agreement with their respective calculated records during both seasons (**Figs. 2(a)** and **(c)**). Therefore the depth-averaged current at St. 2 is representative of tidal currents during the winter but not in the summer.

(2) Raw and non-tidal fitted current velocity spectra

Spectra of the raw and non-tidal fitted current fluctuations at St. 2 for summer and winter were analyzed and are shown in **Figs. 3(a–d)** to verify the observed pattern of the measured and calculated records discussed in the previous section. The raw current indicates the measured current without

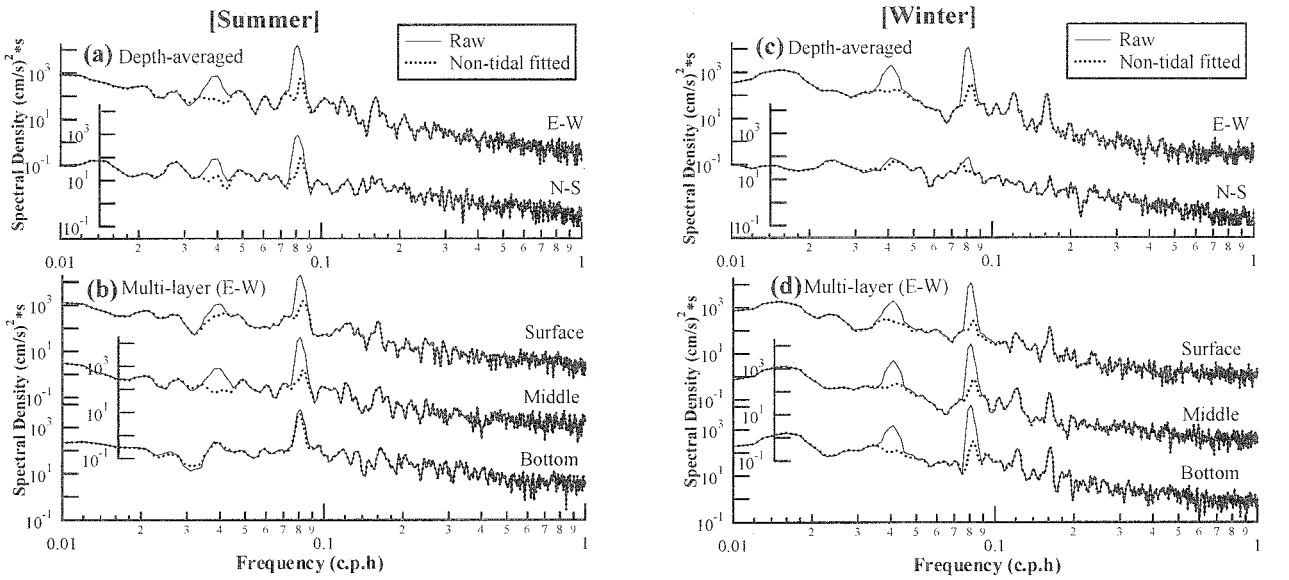

Fig. 3 Frequency spectra of the raw and non-tidal fitted current fluctuations at St.2 for the depth-averaged and E-W component during (a-b) summer and (c-d) winter.

subtracting any fitted constituent records. The non-tidal fitted current was calculated by subtracting the harmonic constituent-based current from the respective raw current. Spectrum analysis was conducted based on the depth-average and multi-layer (surface, middle, and bottom) currents of the E-W component. Each spectrum was calculated using a series of 4,096 data points (10-min. time steps). Since the harmonic analysis used in this study was based on the eight major constituents, energy discrepancies (where they exist) between the raw and non-tidal fitted currents are mainly noticeable on the diurnal and semidiurnal bands. During summer, energy differences between the raw and non-tidal fitted spectra based on the depth-averaged currents show remarkable discrepancies (**Fig. 3(a)**) that are also found in the spectra based on the surface and middle layers (**Fig. 3(b)**). In the bottom layer of the E-W component however, the spectra agreed very well. During winter, on the other hand, energy differences between the raw and non-tidal fitted spectra based on the depth-averaged current and individual layers of the E-W current component shows remarkably similar discrepancy trends at all three depths (**Figs. 3(c)** and **(d)**).

The spectrum analysis confirms the observed pattern, shown in **Fig. 2**, between the calculated depth-averaged and the measured currents in all three layers during summer and winter. To explore the reason for these agreements and disagreements shown in (**Fig. 2**), details of the associated current distributions were assessed and are explained in the following sections.

(3) Vertical structure of horizontal current

The vertical structure of the horizontal current based on baroclinic velocities of St. 2 are considered here to investigate and compare the seasonal current propagation patterns. The baroclinic velocity is calculated by

$$(u', v') = \left(u - \overline{u}_t - \frac{1}{H}\int_{-H}^{0}(u - \overline{u}_t)dz,\right.$$
$$\left. v - \overline{v}_t - \frac{1}{H}\int_{-H}^{0}(v - \overline{v}_t)dz\right) \quad (2)$$

Where H is the water depth; (u, v) is the measured current in an individual layer and $(\overline{u}_t, \overline{v}_t)$ is the time-mean current.

The vertical structure of the horizontal current based on the baroclinic velocity is estimated between 0:00 and 23:00 on September 28, 2007 in summer and December 7, 2006 in winter and is shown in **Fig. 4**. The solid line at the top represents sea level based on Nago observation records. The light and dark areas indicate eastward (northward) and westward (southward) currents, respectively. The circle on the solid lines indicates the time when the TPM Chlorotech sensors were deployed. Current patterns during these deployment times are described in the next section.

Considering the E-W and N-S components together, a southeast (shoreward) current was found in the bottom layer at around 6:00 and 18:00 in summer (**Fig. 4**). After a certain period, at around

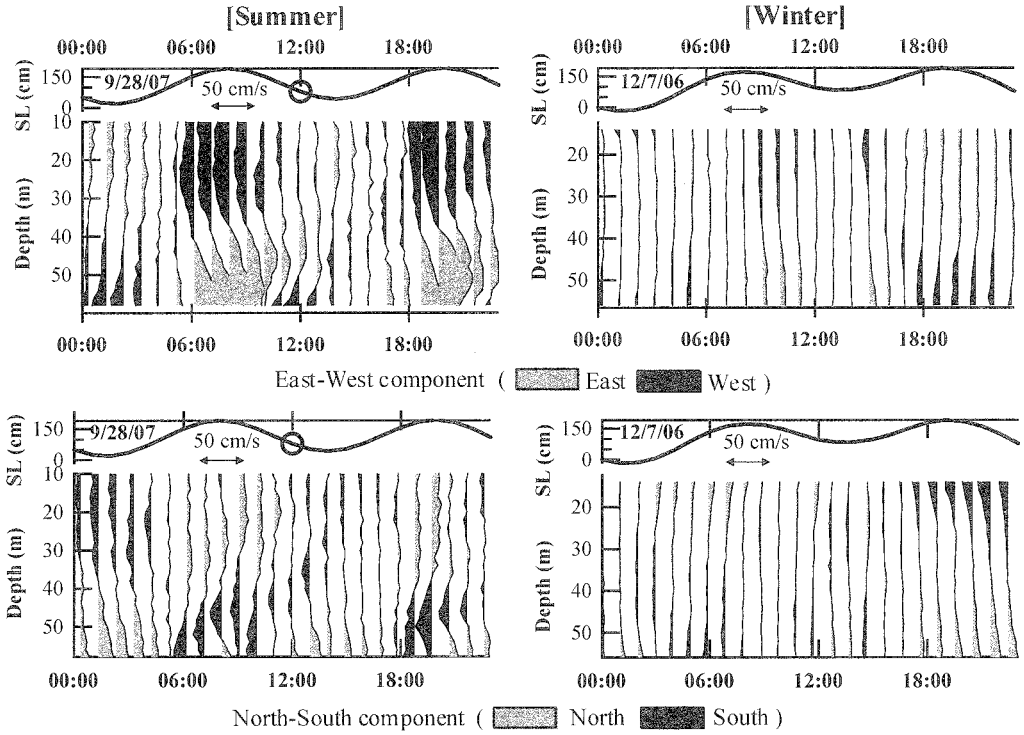

Fig. 4 Vertical structure of horizontal current based on the baroclinic records for St.2 during summer and winter period. Upper panels are the E-W component and bottom panels are the N-S component. Solid line at the top represents the sea level records.

12:00 and 23:00, this southeast current in the bottom layer was replaced by a northwest (offshore) current. The southeast current throughout the vertical profile over time represents an internal wave ray that hits the bottom at around 6:00 and is transmitted toward the surface and downward again after being reflected at the surface. Similarly, the northwest current represents an opposite (180° out of phase) internal wave ray that hits the bottom at around 12:00 and follows a similar transmission and reflection pattern. This phenomenon reveals the existence of an internal tide and its cross-shore propagation at this site during summer. Cross-shore internal tide based propagation patterns with various intensities were also observed in St. 1 and St. 3 during summer and described elaborately in authors' previous paper[6].

Since the internal tides are generated by tidal reflection on the bottom slope, their energy is stronger in the bottom than surface layer. Energy distribution and its transmission were clearly found in the vertical structure of raw current data and explained in a previous study[5]. Internal tide accompanying strong current in the bottom layer during the summer, therefore, caused the discrepancies between the calculated depth-averaged and the measured bottom layer current in St. 2 (**Fig. 2(b)**).

In contrary, stratification patterns were almost absent in the vertical structure of horizontal currents (both E-W and N-S components) in St. 2 during the winter (**Fig. 4**). Similar pattern was also observed in St. 1 and St. 3 and not shown in this paper. Therefore, internal tidal current was almost absent during the winter period and hence, no discrepancies were observed between the calculated depth-averaged and measured bottom layer current in **Fig. 2(d)**.

(4) Vertical Profile of Temperature and Density

In this section, seasonal changes in the vertical profiles of temperature and density are explained with the passage of the internal tide. Temperature (°C) and Density (σ_t) measured vertically using TPM Chlorotech sensors during the summer (September 28, 2007) and winter (December 11, 2006) for each site are shown in **Figs. 5(a** and **b)**, respectively. As shown in **Fig. 5(a)**, pycnocline and thermocline stratifications were observed at all sites during the summer. Even St. 3 shows weak, yet still present, stratification at the bottom.

To justify the present objective only one site St. 2 has elaborately described in this section. The observation time of the TPM records is shown by the circle in **Fig. 4** during summer to identify the corresponding phase of the internal tide in St. 2. Circle was not marked for winter as the internal

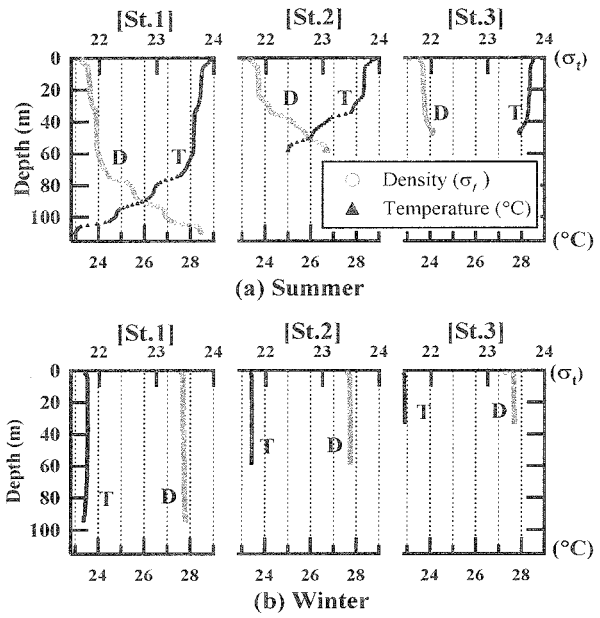

Fig. 5 Depth distribution of temperature and density at Sts.1–3 during (a) summer and (b) winter.

tidal propagation was almost absent. As shown in **Fig. 4** (summer part), the observation time at St. 2 was 12:00 when the internal tide in the bottom layer had just started back offshore after the propagation towards the shore (**Fig. 4**). This internal tide-associated water mass caused a prominent variation in the water density ($\Delta\sigma_t$=1.8) and temperature (ΔT=3.5° C) profiles of St. 2 (**Fig. 5(a)**). Similar relationship was also observed for St. 1 and St. 3 during summer. Conversely, internal tide was almost absent in St. 2 during the winter (**Fig. 4**) and hence, no stratification was observed in temperature and density profiles (**Fig. 5(b)**). Similar homogenous profiles in St. 1 and St. 3 during the winter also indicate the absence of internal tidal propagation in these sites. However, these profiles corroborate the seasonal stratification pattern shown in **Fig. 4**. The above assessments suggest that temperature and density stratification at the bottom is seasonal and associated with the internal tide.

4. CONCLUSION

According to the analysis, the results can be summarized as follows. (1) The calculated depth-averaged records show a good agreement with the measured current records at the surface, middle and bottom layers during the winter but prominent disagreement at the bottom layer during the summer. (2) Frequency spectra of the raw and non-tidal fitted current fluctuations also corroborate the observed pattern. (3) Existence of cross-shore internal tidal current during the summer and their absence during the winter are found to be responsible for the above mentioned agreement at all layers in winter and disagreement at the bottom layer in summer. (4) Variation in temperature and density profile also support the seasonal existence of internal tide in Genka Bay.

Considering the seasonal existence of the internal tide, multi-layer observations should require for an accurate tidal current estimation in Genka Bay. Otherwise, where the internal tide is absent, the one-layer observation should minimize assessment cost and computing time while providing engineers with sufficiently accurate tidal current estimation.

ACKNOWLEDGMENTS: Support for this work was partly provided by Grant-in-Aid for the Disaster Prevention Research of Island Regions (Research representative: Eizo Nakaza). Appreciations are due to graduate and undergraduate students of the Ryukyus University for their cooperation during field observations.

REFERENCES

1. Elshorbagy, W., Azam, M. H. and Taguchi, K.: Hydrodynamic characterization and modeling of the Arabian Gulf, *Journal of Waterway, Port, Coastal, and Ocean Engineering*, ASCE, Vol.132(1), pp.47-56, 2006.

2. Espino, M., Maidana, M. A., Sanchez-Arcilla, A. and German, A.: Hydrodynamics in the Huelva Estuary: Tidal model calibration using field data, *Journal of Waterway, Port, Coastal, and Ocean Engineering*, ASCE, Vol.133(5), pp.313-323, 2007.

3. Yoshida, M. and Takasugi, Y.: Influence of artificial topographical transformation on the tide in the Seto Inland Sea, Japan, *Journal of Waterway, Port, Coastal, and Ocean Engineering*, ASCE, Vol.131(2), pp.62-68, 2005.

4. Ward, N. D., Gebert, J. A. and Weggel, J. R.: Hydraulic study of the Chesapeake and Delaware Canal, *Journal of Waterway, Port, Coastal, and Ocean Engineering*, ASCE, Vol.135(1), pp.24-30, 2009.

5. Nakaza, E., Rahaman, S. M. B., Kitamura, Y., Pawlak, G. and Tsukayama, S. : Cross-shore internal waves in Zanpa coastal region of Okinawa Island, *Journal of Waterway, Port, Coastal, and Ocean Engineering*, ASCE, Vol.132(1), pp. 36-46, 2006.

6. Rouf, M. A., Nakaza, E., Kudaka, R. and Liliane, K.: Characteristics of the internal tide and its associated cooling system in Genka Bay, Okinawa, Japan, *Japan Society of Civil Engineering Journal*, JSCE, (In print).

7. Duda, T. F., Lynch, J. F., Irish, J. D., Beardsley, R. C., Ramp, S. R., Ching-Sang, C., Tang, T. Y. and Ying-Jang, Y.: Internal tide and nonlinear internal wave behavior at the continental slope in the northern south China Sea. *IEEE Journal of Oceanic Engineering*, Vol.29(4), pp.1104-1130, 2004.